



Correlation between the ionic conductivity and the relaxation mechanisms during the 436 K- transition in nitrate salt RbNO_3 : analysis by impedance spectroscopy

Khaled Hammami ¹, Taher Mhiri ¹, Xavier Le Goff ² and Khaled Jarraya ^{1*}

¹Laboratoire Physico-Chimie de L'État Solide, Faculté des Sciences
BP 1171, 3000 Sfax, Tunisie.

²Laboratoire Diffusion – Diffraction, UMR 5257 Institut de Chimie Séparative de Marcoule
BP 17171, 30207 Bagnols, France.

*Corresponding author: khaledjarraya@yahoo.fr

Tel.: +216 98 414 144

Fax: +216 74 27 44 37.

Abstract.

The measurements of the complex impedance Z^* , the conductivity σ , the dielectric permittivity ϵ'_r , and the complex modulus M^* were carried out on the RbNO_3 compound at frequencies ranging between 1 and 10^6 Hz. In fact, the conductivity follows the Arrhenius law in the different temperature ranges $\sigma T = \sigma_0 \exp(-\Delta E \sigma / kT)$. Actually, the resulting curve shows an anomaly between 425 and 436 K and a sudden increase in conductivity to 436 K causing σ to pass from $1.6 \times 10^{-6} \Omega^{-1} \cdot \text{cm}^{-1}$ to $9.3 \times 10^{-5} \Omega^{-1} \cdot \text{cm}^{-1}$. This behavior clearly confirms the ionic character of the phase transition at this temperature. The main objective of this research study is to show the correlation between the ionic conductivity and the relaxation mechanisms during this transition.

Keywords: Impedance spectroscopy; Ionic conductivity; Modulus analysis; Permittivity; Dielectric relaxation.

Council for Innovative Research

Peer Review Research Publishing System

Journal: Journal of Advances in Chemistry

Vol. 10, No. 3

editorjaonline@gmail.com

www.cirjac.com



1. INTRODUCTION

Just like all the compounds of the alkali nitrates family [1, 2], RbNO₃ is crystallized in the trigonal system P3₁. The material under investigation is known to have four stable phase transitions at atmospheric pressure [3]. Actually, its structure has been solved by neutron diffraction [3] and confirmed by X-ray diffraction single-crystal investigations [1].

The research studies of Sadananda [4] on the variation of ionic conductivity with temperature on the single crystals of RbNO₃ have been an attempt to show that there are variations in the conductivity corresponding to these phase transitions. However, no exhaustive studies on the electrical properties during the transition detected at 436 K, especially the ionic conductivity, have been reported. So the originality of the present study is to look up the electrical properties and show the importance of the conductivity as well as the conduction property of the material in this transition. Likewise, by further studying the real relative dielectric permittivity ϵ'_{r} , and complex modulus M^* , we have been able to show the contributions of the polarization phenomena during this transition.

2. MATERIALS AND METHODS

The RbNO₃ compound was obtained from an aqueous solution of a mixture of Rb₂CO₃ and HNO₃. The resulting solution was kept under ambient conditions, which allowed slow evaporation. Fourteen days later, we obtained transparent and lamellar-shaped colorless crystals with a size of about (0.25 x 0.25 x 0.30) mm³. The crystals were severely selected from using a polarizing microscope for different analysis.

The electrical properties were collected under stagnant air atmosphere. The measurements of the complex dielectric permittivity ($\epsilon^* = \epsilon' - j\epsilon''$) were performed over a frequency interval of 1–10⁶ Hz and in a temperature range of 393–469 K. To cover the above frequency range, a Novocontrol spectrometer integrating an ALPHA dielectric interface was employed with a precision in $\tan\delta = \epsilon''/\epsilon' = 10^{-5}$. In these experiments, the temperature was controlled by a nitrogen jet (QUATRO from Novocontrol) with a temperature error during every single sweep in frequency of ± 0.1 K.

3. RESULTS AND DISCUSSION

The study of the variation of ionic conductivity with temperature on RbNO₃ single crystals showed that only the transition detected at 436 K was associated with a maximum variation of the conductivity.

3.1. Impedance analysis

Single crystal RbNO₃ has been investigated by impedance spectroscopy and conductivity phenomena in an attempt to understand the relaxation mechanisms so as to find a correlation between the conductivity and dielectric relaxation processes.

The evolution of the curves, $-Z''$ versus Z' , between 393 and 433 K of the RbNO₃ compound are illustrated in Figure-1. It can be noted that the Cole-Cole model is rather valid in representation ϵ'' (ϵ') than in representation Z'' (Z') and the material under study is proven to follow the Cole–Cole law. The difference between the Cole–Cole and the Debye law is also determined ($\alpha = 0.12$) from this figure. The bulk ohmic resistance relative to a given temperature can be calculated from the intercept on the real axis of the zero phase angle extrapolation of the highest-frequency curve. The impedance curves $-Z''$ as a function of Z' shows a thermal behavior of the material resistance, which in turn confirms the conducting property of our compound.

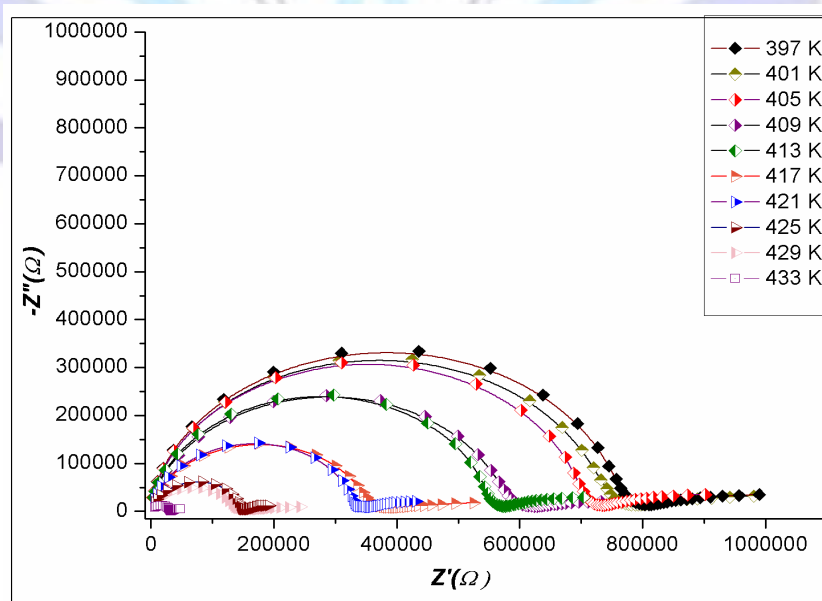


Fig.1. Variation of the imaginary part $-Z''$ versus Z' , for RbNO₃ at various temperatures.

The RbNO₃ compound's evolution of the conductivity versus inverse temperature $\log_{10}(\sigma T) = f(1000/T)$ between 393 and 469 K, is shown in Figure (2-a). The experimental points demonstrate the Arrhenius law in various temperature ranges $\sigma T = \sigma_0 \exp(-E\sigma/kT)$ where σ_0 is a pre-exponential factor and $E\sigma$, k and T are the activation energy for conduction process, Boltzmann's constant and the absolute temperature, respectively. The resulting curve indicates an anomaly between 425 and 436 K. Regarding the activation energy for the conduction process ($E\sigma$), which reached 0.76 eV in this temperature range, it was extracted by the slope of the straight line in the $\log(\sigma T)$ against reciprocal temperature $1/T$ plot.

Moreover, the increase in temperature causes a sudden jump in conductivity at 436 K. Indeed, from the temperature $T = 425$ K to $T = 436$ K, σ increases from $1.6 \times 10^{-6} \Omega^{-1} \cdot \text{cm}^{-1}$ to $9.3 \times 10^{-5} \Omega^{-1} \cdot \text{cm}^{-1}$. This obviously substantiates the presence of a phase transition at 436 K. In fact, for the ionic conductors (IC), the conductivity can attain $10^{-5} \Omega^{-1} \cdot \text{cm}^{-1}$ while for the superionic conductors (SIC), it is at least equal to $10^{-4} \Omega^{-1} \cdot \text{cm}^{-1}$. The main difference between these two groups of materials can be attributed to the activation energy ($\Delta E\sigma$). In the case of (SIC), $\Delta E\sigma$ is less than 0.4 eV, whereas in (IC), the commonly observed values [5, 6] vary between 0.6 and 1.2 eV.

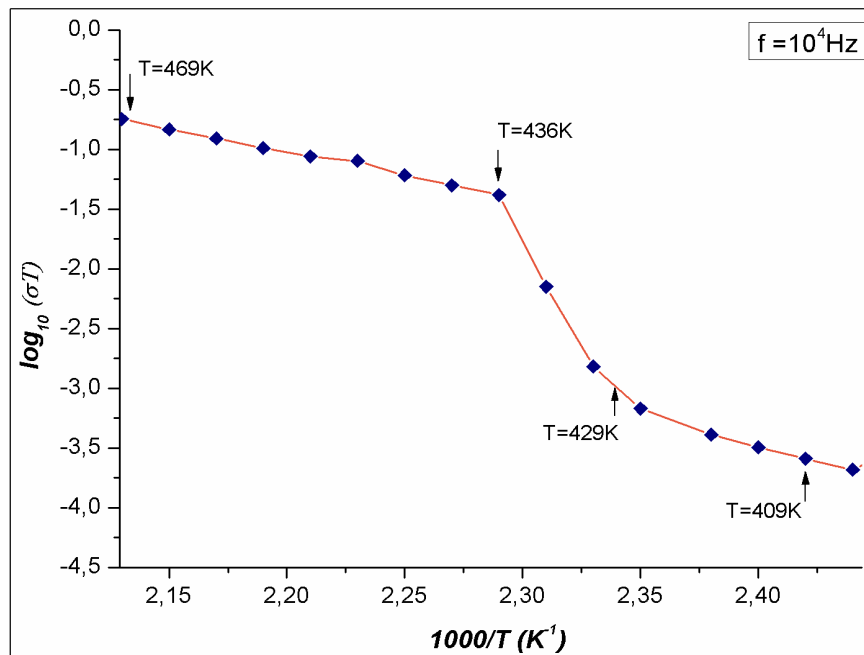


Fig.2a. Temperature dependencies of $\log(\sigma T)$ versus $(1000 / T)$ for RbNO₃.

Figure (2-b) shows the variation of conductivity as a function of frequency logarithmic, at several temperatures. From this growth, we can deduce an evolution in the conductivity values. This suggests that more than one conduction mechanism can be responsible of this conductivity in this material. A good agreement between experimental and theoretical fitting is observed [7]. Depending on the measurement temperature a dc plateau precedes an increase of conductivity with frequency.

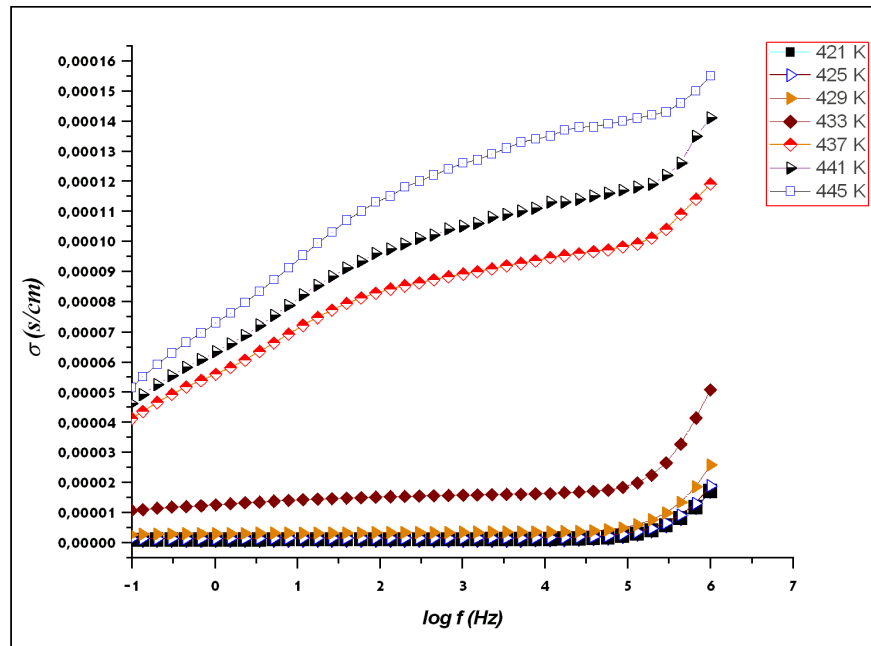


Fig.2b Variation of conductivity as a function of frequency logarithmic, at several temperatures.

3.2. Modulus spectroscopy analysis

The dielectric spectroscopy in the frequency range of mHz to GHz is an important tool to study many relaxation processes in solids [8-10]. Figure 3 represents the variation of the imaginary part Z'' as a function of frequency. In fact, the curve $-Z'' = f(\log f)$ demonstrates that the relaxation frequency shifts to higher frequencies and its intensity decreases with the increase in temperature. This behavior leads to the conclusion that the ionic species are becoming increasingly mobile at high temperature [11].

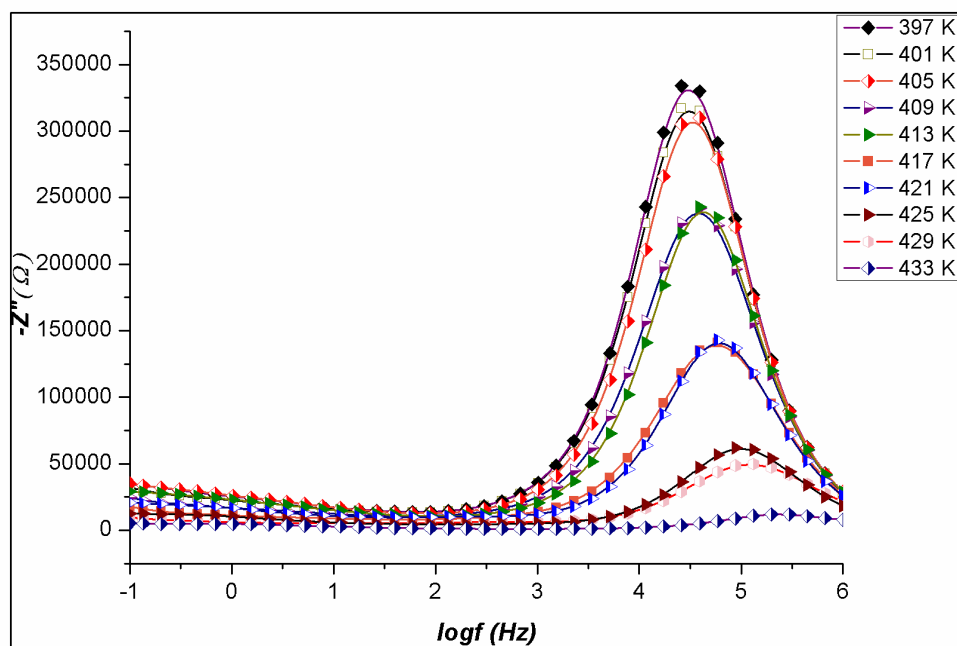


Fig.3 Variation $-Z''$ versus frequency at different temperatures.

Aiming at the determination of the relaxation time of conductivity of the compound under study, the use of the complex modulus formalism is an alternative approach to investigate the electrical response of materials that present some degree of ionic conductivity:

$$M^*(w) = 1/\varepsilon^* = jwC_oZ^*(w)$$

This formalism is particularly suitable to detect phenomena as electrode polarization [12] and bulk property as average conductivity relaxation times τ [13-15].

When the electrical behavior of RbNO₃ was studied by this formalism, we have firstly made sure that the polarization phenomena at the electrodes were characterized by a minor contribution in M^* . Indeed, the variation of the real component M' of the complex modulus at different temperatures as a function of the frequency (Figure-4) has shown that M' reaches a constant value at high frequency with the right ($M' = 1/\varepsilon'_{\infty}$) as asymptote, in the fields of swept temperature and frequency, at all temperature investigated. This indicates that the electrode polarization phenomena make a negligible contribution to M^* [16] and may be ignored when the electrical data are analyzed in this form [17].

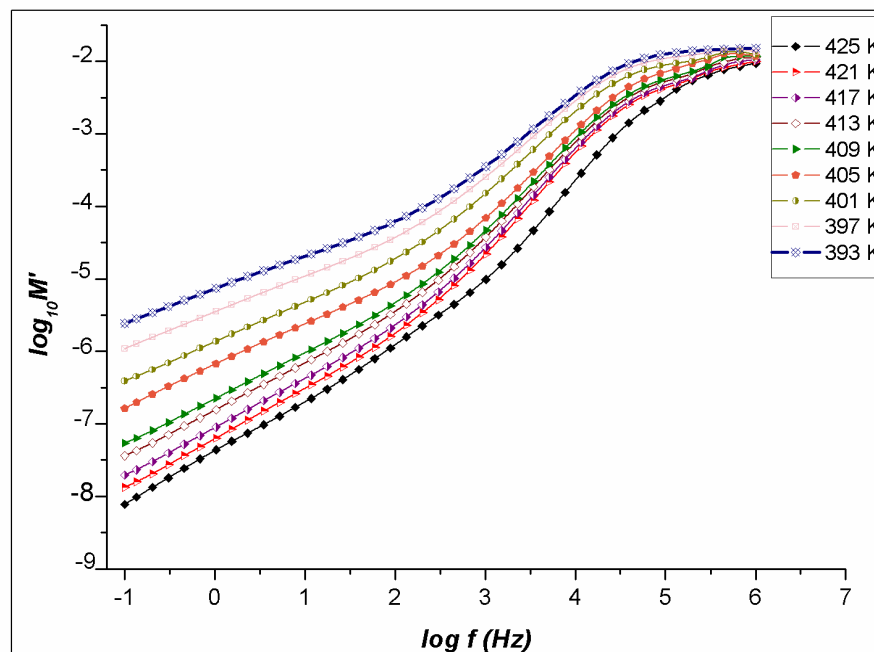


Fig.4. Plots of $\log M'$ versus $\log (f)$ for RbNO₃ at various temperatures.

The curves representing the variation of the imaginary part of M^* modulus normalized as a function of $\log (f)$ for different temperatures are reported in Figure 5. They appear as peaks in the asymmetric relaxation maxima and move towards higher frequencies with the increase in temperature [18, 19]. To this maximum of M'' corresponds a characteristic frequency f_p . This behavior is in line with the non-exponential approach of electrical functions, which are defined by the empirical stretched Kohlrausch function $\phi(t) = \exp[-(t/\tau)^\beta]$.

Regarding the full width at half maximum (FWHM) of the M''/M''_{\max} , it is found to be close to that of a Debye peak (1.14 decade) [18], from which results a parameter value of Kohlrausch β that is smaller than 1. This can be accredited to the existence of time relaxation distribution in the material, which is an interpretation that has been adopted for numerous solid electrolytes [20-24].

The f_p peak frequency corresponding to maximum in M''/M''_{\max} as a function of logarithmic of frequency, shown in Figure 5, is typically correlated to the average conductivity relaxation time or most probable ion relaxation time τ ($\tau = 1/2\pi f_p$). As for the $\log(\tau T)$ as a function of reciprocal temperature $1/T$, it is shown in Figure 6.

Besides, the experimental data are well described by the expression type Arrhenius, given as follows: $\tau T = \tau_0 \exp(E\tau/kT)$

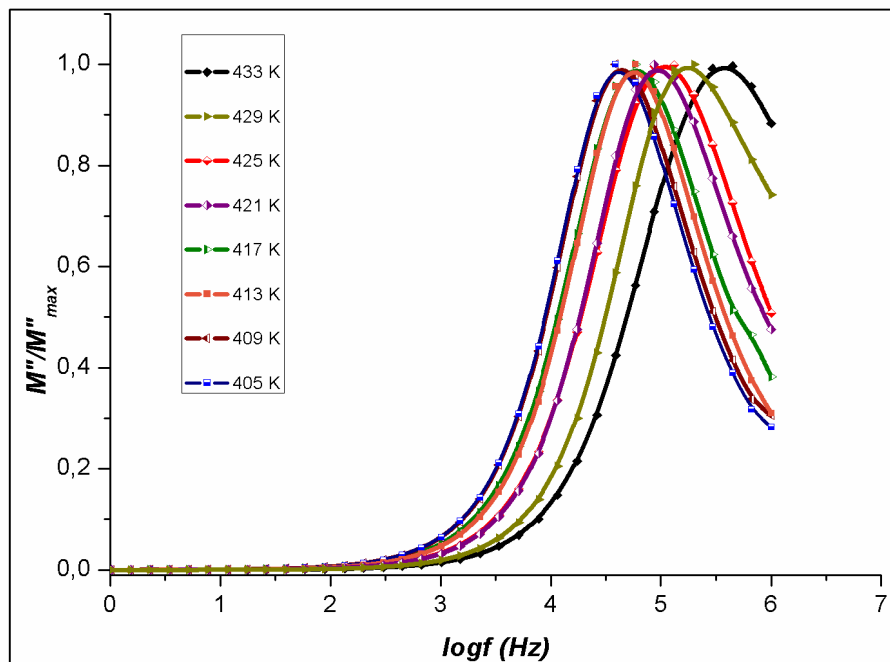


Fig.5. Variation of M''/M''_{max} versus $\log(f)$.

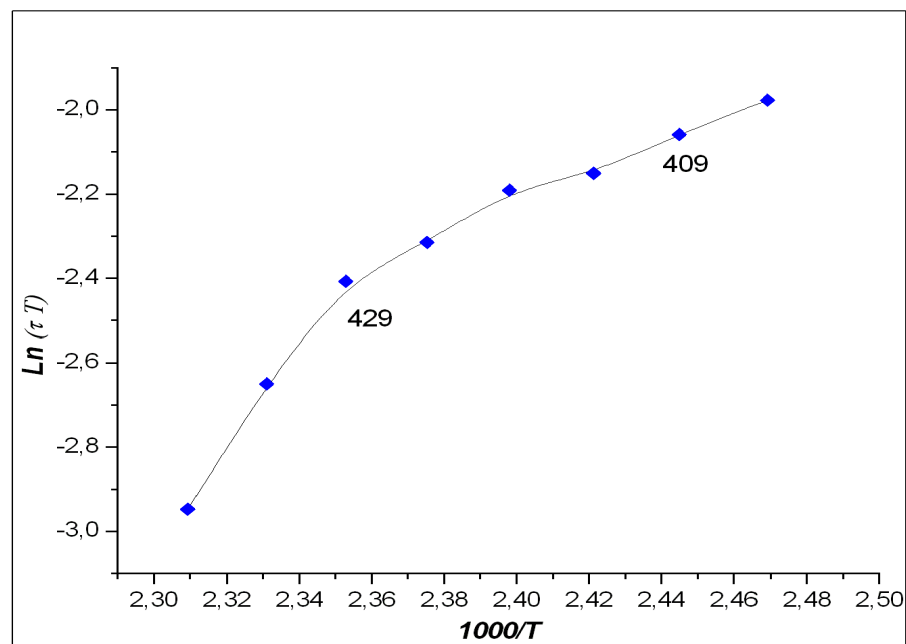


Fig.6. Arrhenius plot of relaxation time of the sample: The $\log(\tau T)$ as a function of reciprocal temperature $1/T$,

where τ_0 is the pre-exponential factor and E_τ is the activation energy for the conductivity relaxation. The activation energy of the relaxation process E_τ was extracted by the slope of the straight line in the $\log(\tau T)$, reaching 0,95 eV (Figure 6), which is different from E_σ value. The latter represents the activation energy for the conduction process that is calculated from relaxation time plots (see Figure-2-a). However, Réau et al. [15] and Naili et al. [25] have suggested that whether E_σ and E_τ are similar or equal, this is further evidence for ionic-hopping mechanism for transport. So far, it is worthy to note that all these observations about the energy values may be considered as a proof for ionic conduction in

the sample. Then, a conduction mechanism type can be explained by the presence of a correlation between the ionic conductivity and the relaxation phenomenon during this transition.

Figure (7-a), shows the frequency evolution of the dissipation factor ($\tan\delta$). The values of ($\tan\delta$) are relatively important, indicating a significant contribution of the conductivity in this material. The dielectric loss presents a maximum then it decreases.

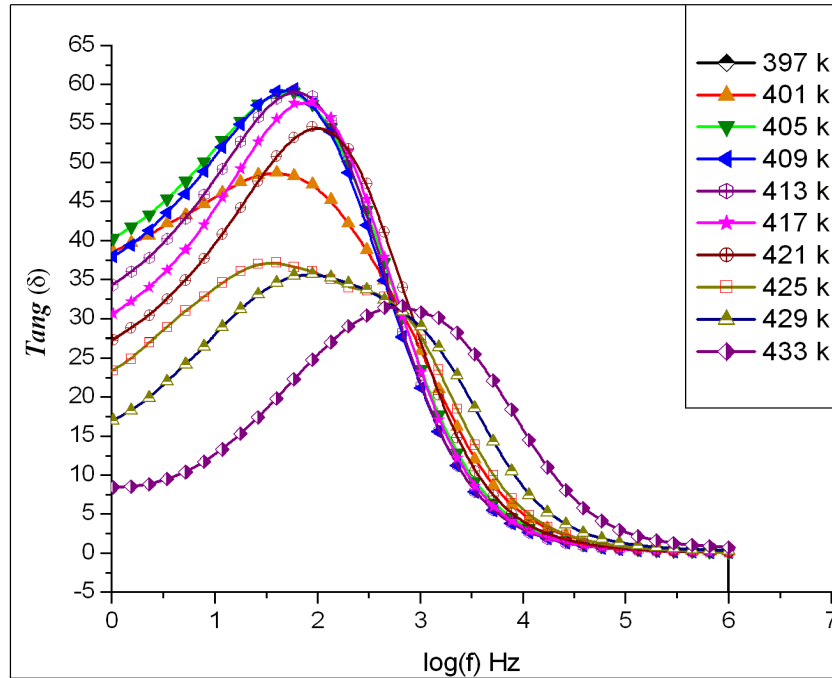


Fig.7a. Thermal evolution of the dissipation factor δ as a function of temperature, for different frequencies.

The position of $\tan\delta$ maximum depends on the frequency; it shifts to higher temperatures with the increase in the frequency.

The important evolution of the permittivity as a function of frequency is attributed to the relaxation phenomenon, i.e. the amortization of reorientation movements that are causing the dipole moment.

Figure (7-b) represents the variation of the real part Z' and imaginary part Z'' of the impedance Z for the temperature $T = 425$ K, as a function of $\log(\omega)$. We note that the maximum of $Z''(\omega)$ corresponds to the inflection point of $Z'(\omega)$. The same behavior of $Z'(\omega)$ and $Z''(\omega)$ was observed in the temperature range 397-433 K (see Figure(7-c)).

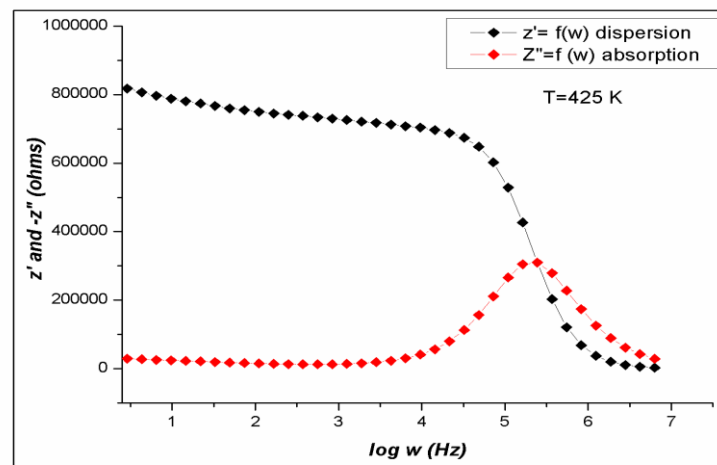


Fig.7b. Variation as a function of $\log(\omega)$, the real part of Z' and of the imaginary part Z'' of the sample for the temperature $T = 425$ K.

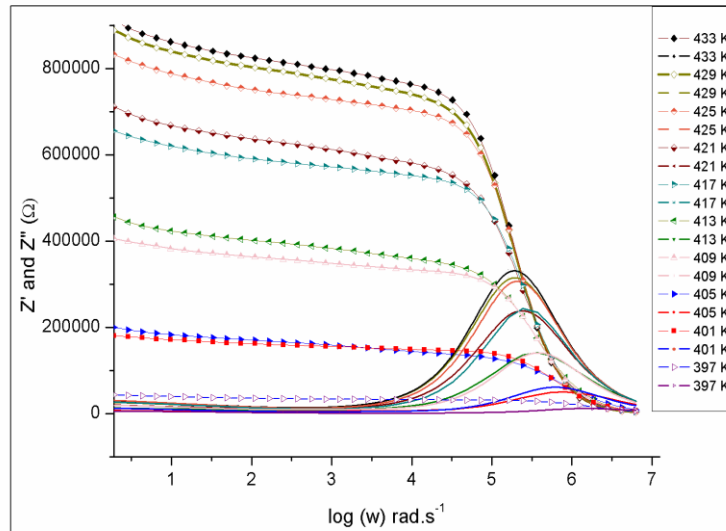


Fig.7c. Behavior of $Z'(\omega)$ and $Z''(\omega)$ in the temperature range 397-433 K for RbNO3.

Indeed in the Debye model, the position (frequency) of the maximum of $\tan\delta$ does not coincide with the position of the maximum of $Z''(\omega)$ [26]. The result we reached is not surprising. On the other hand, the behavior of the relaxation frequency as a function of temperature shows that when approaching the transition temperature T_r , the minimum of frequency is obtained, therefore a longer time ($\tau = 1 / 2\pi f\tau$) is necessary for the relaxation of the material after its modification [27]. The lattice relaxation is probably correlated to the process of intrinsic polarization of the material. In this temperature range, the displacement could be coupled with the lattice dynamics [28].

It is worthwhile to mention that Figure-8 has shown the evolution of permittivity as a function of temperature at different frequencies.

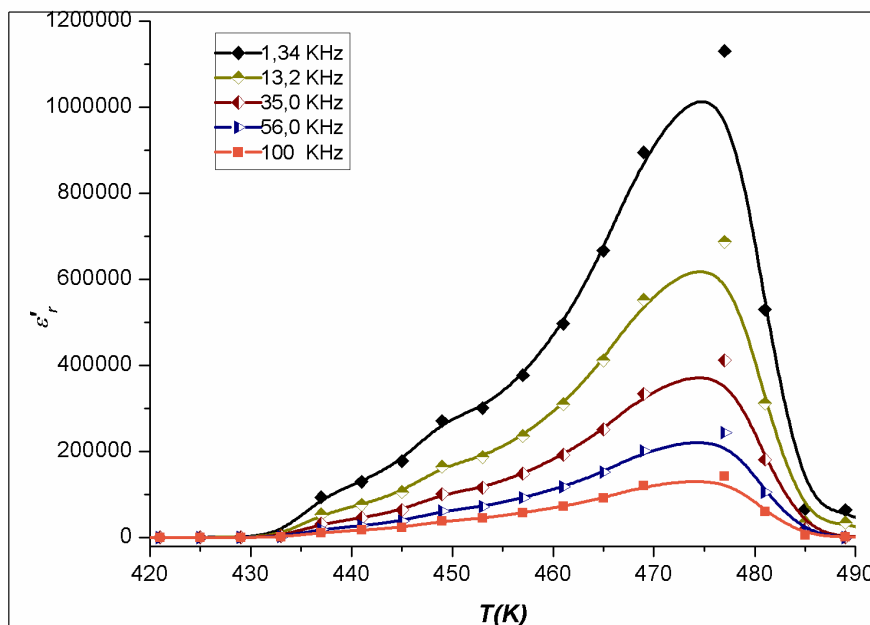


Fig.8. Temperature dependence of the permittivity $\epsilon'r$ as a function of temperature, for different frequencies.

Indeed, the evolution of $\epsilon'r$ for various frequencies has shown a significant variation of the permittivity in this material. It seems to be very low between room temperature and 428 K, which rules out the possibility of any major structural change inducing polar evolution in the system. Above this temperature, and when reducing the frequency (from 1.34 kHz to 100 kHz), $\epsilon'r$ increases gradually from 458 K to reach a peak at 473 K. The maximum $\epsilon'max$ decreases when



the frequency increases which characterize an important dispersion linked to the presence of conductivity in this material. The dielectric anomaly in the permittivity can characterize a structural transition in the salt [29]. Consequently, two polarization mechanisms are possible and the real part of dielectric constant can be presented as:

$$\epsilon' r = \epsilon' r (\text{latt}) + \epsilon' r (\text{carr})$$

where $\epsilon' r(\text{latt.})$ represents the lattice response related to permanent dipole orientation, and $\epsilon' r(\text{carr.})$, represents the conductivity relaxation. The second contribution is slightly linked to the frequency, especially in the low frequency domain. This part of the permittivity characterizes the conductivity mechanisms [11, 17].

The orientational disorder and the increased rotation of the nitrate ion are supposed to be the main factors responsible for the abrupt change in conductivity and dielectric permittivity ϵ [30]. However, the important values of the permittivity at low frequency, below this temperature ($T = 436$ K) could be due to the cumulative contributions of different phenomena in the crystal such as (i) ionic polarization (ii) orientation polarization.

4. CONCLUSION

We have determined the electrical properties of RbNO₃ compound over a wide frequency range, as a function of temperature. The impedance curves $-Z'' = f(Z')$ of the studied material obey the Cole - Cole law, showing the conducting property of the compound.

Besides, the transition detected at 436 K was found to be dominant and associated with a maximum variation of the conductivity. It goes from $1.6 \times 10^{-6} \Omega^{-1} \cdot \text{cm}^{-1}$ to $9.3 \times 10^{-5} \Omega^{-1} \cdot \text{cm}^{-1}$, thus confirming the presence of a phase transition at this temperature. We detect a difference between the value of activation energy for conduction $E\sigma = 0.76$ eV and that for the relaxation process $E\tau = 0.95$ eV. This leads to the conclusion that there is a correlation between the phenomenon of ionic conduction and dielectric relaxation. We have also shown that the contributions of polarization phenomena occurring during this transition at the electrodes are negligible.

REFERENCES

- [1] C. Dean, T.W. Hambley and M.R. Show, *Acta Cryst. C*, 40, (1984), 1512-1515.
- [2] J. Pohl, D. Pohl and G. Adiwidjaja, *Acta Crystallogr., Sect. B* 48, (1992), 160-166.
- [3] B.W. Lucas, *Acta Cryst., C* 39, (1983), 1591-1594.
- [4] A. Sadananda Chary, S. Narender Reddy and T. Chiranjivi, *Solid State Ionics*, 31, (1988), 27-30.
- [5] Ph. Colomban, J.C. Badot, M. Pham-Thi and A. Novak, *Phase Transit.*, 14, (1989), 55-59.
- [6] Ph. Colomban, *Proton Conductors: Solids, Membranes, and Gels Materials and Devices*, Cambridge University Press, 1992.
- [7] S. Lanfredi, P. S. Saia, R. Lebullenger and A. C. Hernandez, *Solid State Ionics*, 146, (2002), 329-339.
- [8] A. K. Jonscher, *Nature*, 267, (1977), 673-679.
- [9] A. K. Jonscher, *Dielectric Relaxation in Solids*, (Chelsea dielectric press, London. 56-67 1983).
- [10] A. K. Jonscher, *Dielectric Relaxation in Solids* (Chelsea Dielectric Press, London, 1987). See also A. K. Jonscher, *Universal Relaxation Law* (Chelsea Dielectric Press, London, 1996), and more recently A. K. Jonscher, *J. Phys. D* 32, R57 (1999).
- [11] M.D. Ingram, C. T. Moynihan and A.V. Lesikar. *J. Non Cryst. Solids*, 38-39, (1980), 371-376.
- [12] D.P. Almond and A. R. West, *Solid State Ionics*, 11, (1983), 57-64.
- [13] R. Gerhardt and *J. Phys. Chem. Solids*, 55, (1994), 1491-1506.
- [14] J.M. Bobe, J. M. Re'au and J. Senegas, M. Poulain, *Solid State Ionics*, 82, (1995), 39-52.
- [15] J.M. Re'au, X. Y. Jun, J. Senegas, Ch. Le Deit and M. Poulain, *Solid State Ionics*, 95, (1997), 191-199.
- [16] S.M. Haile, G. Lentz, K.D. Kreuer and J. Maier, *Solid State Ionics*, 77, (1995), 128-134.
- [17] N. Zouari, K. Jaouadi and T. Mhiri, *Journal of Solid State Ionics*, 177, (2006), 237-244.
- [18] S.W. Martin and C. A. Angell, *J. Non-Cryst. Solids*, 83, (1986), 185-207.
- [19] K.L. Ngai and S. W. Martin, *Phys. Rev. B*, 40, (1989), 10550-10554.
- [20] H.K. Patel and S. W. Martin, *Phys. Rev. B*, 45, (1992), 10292-10299.
- [21] H. Liu, G. K. Sundar and C.A. Angell, *Journal of Solid State Ionics*, 18-19, (1986), 442-448.
- [22] A. Pimenov, P. Lunkenheimer, H. Rall, R. Kohlhaas and A. Loidl, *Physical Review*, 1996, V54, N1, 676-684.



- [23] M. Hodge, K.L. Ngai and C.T. Moynihan, *J. Non-Cryst. Solids*, 351, (2005), 104-115.
- [24] J. R. Macdonald, *J. Phys. Chem., B* 111, (2007), 7064-7072.
- [25] H. Naili, N. Zouari, T. Mhiri A. Daoud, *J. Mol. Struct.*, 519, (2000), 143-151.
- [26] V.V. Daniel, *Dielectric relaxation*, Acad. Press, Londres, 1967.
- [27] M.A. K Abdelhalim and M. M. Mady, M. M. Ghannam
International Journal of the Physical Sciences, Vol. 6 (23), (2011), 5487-5491.
- [28] M.E. Lines, A.M. *Glass Principles and Applications of Ferroelectrics and Related Materials*, Clarendon Press. Oxford, 1977.
- [29] D. Hongliang, Z. Wancheng, L. Fa, Z. Dongmei, Q. Shaobo and P. Zhibin
J. Appl. Phys., 105, (2009), 124104-124110.
- [30] C.J. Leedecke and R.E. Loehman, *J. Am. Ceram. Soc.*, 63, (1980), 190-193.

FIGURE CAPTIONS

- Fig.1. Variation of the imaginary part $-Z''$ versus Z' , for RbNO_3 at various temperatures.**
- Fig.2a. Temperature dependencies of $\log(\sigma T)$ versus $(1000 / T)$ for RbNO_3 .**
- Fig.2b Variation of conductivity as a function of frequency logarithmic, at several temperatures.**
- Fig.3 Variation $-Z''$ versus frequency at different temperatures.**
- Fig.4. Plots of $\log M'$ versus $\log(f)$ for RbNO_3 at various temperatures.**
- Fig.5. Variation of M'' / M''_{max} versus $\log(f)$.**
- Fig.6. Arrhenius plot of relaxation time of the sample: The $\log(\tau T)$ as a function of reciprocal temperature $1/T$,**
- Fig.7a. Thermal evolution of the dissipation factor δ as a function of temperature, for different frequencies.**
- Fig.7b. Variation as a function of $\log(\omega)$, the real part of Z' and of the imaginary part Z'' of the sample for the temperature $T = 425$ K.**
- Fig.7c. Behavior of $Z'(\omega)$ and $Z''(\omega)$ in the temperature range 397-433 K for RbNO_3 .**
- Fig.8. Temperature dependence of the permittivity ϵ_r as a function of temperature, for different frequencies.**